

## Comparison of LIBS results on ITER-relevant samples obtained by nanosecond and picosecond lasers



P. Paris<sup>a</sup>, J. Butikova<sup>b</sup>, M. Laan<sup>a</sup>, A. Hakola<sup>c</sup>, I. Jõgi<sup>a</sup>, J. Likonen<sup>c</sup>, E. Grigore<sup>d</sup>, C. Ruset<sup>d</sup>

<sup>a</sup> Institute of Physics, University of Tartu, Tartu 50411, Estonia

<sup>b</sup> Institute of Solid State Physics, University of Latvia, Riga LV-1063, Latvia

<sup>c</sup> VTT Technical Research Centre of Finland Ltd., 02044 VTT, Finland

<sup>d</sup> National Institute for Lasers, Plasma and Radiation Physics, Bucharest 077125, Romania

### ARTICLE INFO

#### Keywords:

ITER-relevant coatings  
LIBS diagnostics  
Detection of hydrogen isotopes  
Elemental depth profiles  
Temperature of laser-produced plasma

### ABSTRACT

ITER foresees applying laser induced breakdown spectroscopy (LIBS) as a tool for quantitative assessment of fuel retention in the first walls. One open problem related to LIBS application is the choice of the laser type. Here we compare two Nd/YAG lasers with different pulse durations, 0.15 and 8 ns, working at  $\lambda = 1064$  nm for LIBS studies of samples with D-doped W/Al coatings of  $\approx 3$   $\mu\text{m}$  thickness (Al is used as a proxy of Be) on Mo. Low pressure argon was used as a background gas. Experiments were done in conditions where other factors (broadening of spectral lines, signal-to-noise ratio, limited thickness of coatings etc.) did not shadow the effect of laser pulse duration. For these reasons, low pressure argon was used as the background gas and fluences were kept at comparatively low values. Spectra of laser-produced plasma were recorded as a function of the number of laser pulses.

Partially overlapping lines of hydrogen isotopes were fitted with Voigt contours, intensities were fitted and depth profiles of deuterium were reconstructed. The relative standard error of curve-fitting of spectra recorded with the laser of shorter pulse duration was two times smaller than that recorded by the longer pulse laser. The electron density was found from the Stark broadening of  $H_{\alpha}$  line of the laser-produced plasma and the electron temperature of plasma was found on the basis W and Mo lines.

It was found that in the case of ps laser an acceptable accuracy of the detection of deuterium was possible at considerably lower values of fluence. Steps needed for comparison of ps and ns lasers in ITER-relevant conditions were discussed.

### 1. Introduction

The ITER strategy foresees applying laser induced breakdown spectroscopy (LIBS) for quantitative in situ diagnostics of fuel retention in the first walls during maintenance breaks. Quantitative information could be obtained by calibration-free LIBS, CF LIBS, where the elemental composition of a sample is determined on the basis of the accurate knowledge of the electron temperature  $T_e$  and the electron density  $n_e$  [1]. To this end, reliable detection of spectral lines of hydrogen isotopes as well as those of the host material is required.

Determining fuel retention by LIBS is hampered by two main issues. First, at high densities of charge carriers in a laser-created plasma,  $H_{\alpha}$  and  $D_{\alpha}$  lines are partly overlapping due to the Stark broadening. Long delay times between the laser pulse and the beginning of data acquisition,  $t_d$ , reduces the overlap because the density of charge carriers in plasma decreases with  $t_d$ . However, the signal-to-noise ratio, S/N, decreases simultaneously with  $t_d$ . Secondly, stronger lines of the target material are influenced by self-absorption and at larger values of  $t_d$  the intensity of lines with lower self-absorption has a low S/N ratio. These are the main reasons triggering the search for alternative solutions for

reliable recording of LIBS spectra.

Most fusion-related LIBS measurements are carried out by using single-pulse lasers with nanosecond pulse duration. However, studies related to hydrogen isotopes detection [2] show that the nanosecond double-pulse LIBS improves the S/N ratio. Besides, some studies [3,4] indicate that using lasers with a shorter pulse duration would be advantageous for determining the surface characteristics and retained fuel depth profiles of the analyzed samples.

The aim of the present study is to compare the effect of different pulse durations on LIBS results of ITER-relevant samples. Other experimental conditions, e.g. pressure and fluence, were selected in the way which showed most clearly the effect of pulse duration. The study is a necessary groundwork for following studies at atmospheric pressure relevant for diagnostics during the maintenance breaks.

### 2. Materials and methods

The investigated samples simulating the co-deposits encountered on ITER walls were D-doped W/Al coatings (Al is used as a proxy of Be) on Mo. Depending on the position in the ITER wall, the co-deposits can be

<https://doi.org/10.1016/j.nme.2018.11.018>

Received 30 July 2018; Received in revised form 20 November 2018; Accepted 22 November 2018

Available online 30 November 2018

2352-1791/© 2018 The Authors. Published by Elsevier Ltd. This is an open access article under the CC BY license (<http://creativecommons.org/licenses/by/4.0/>).

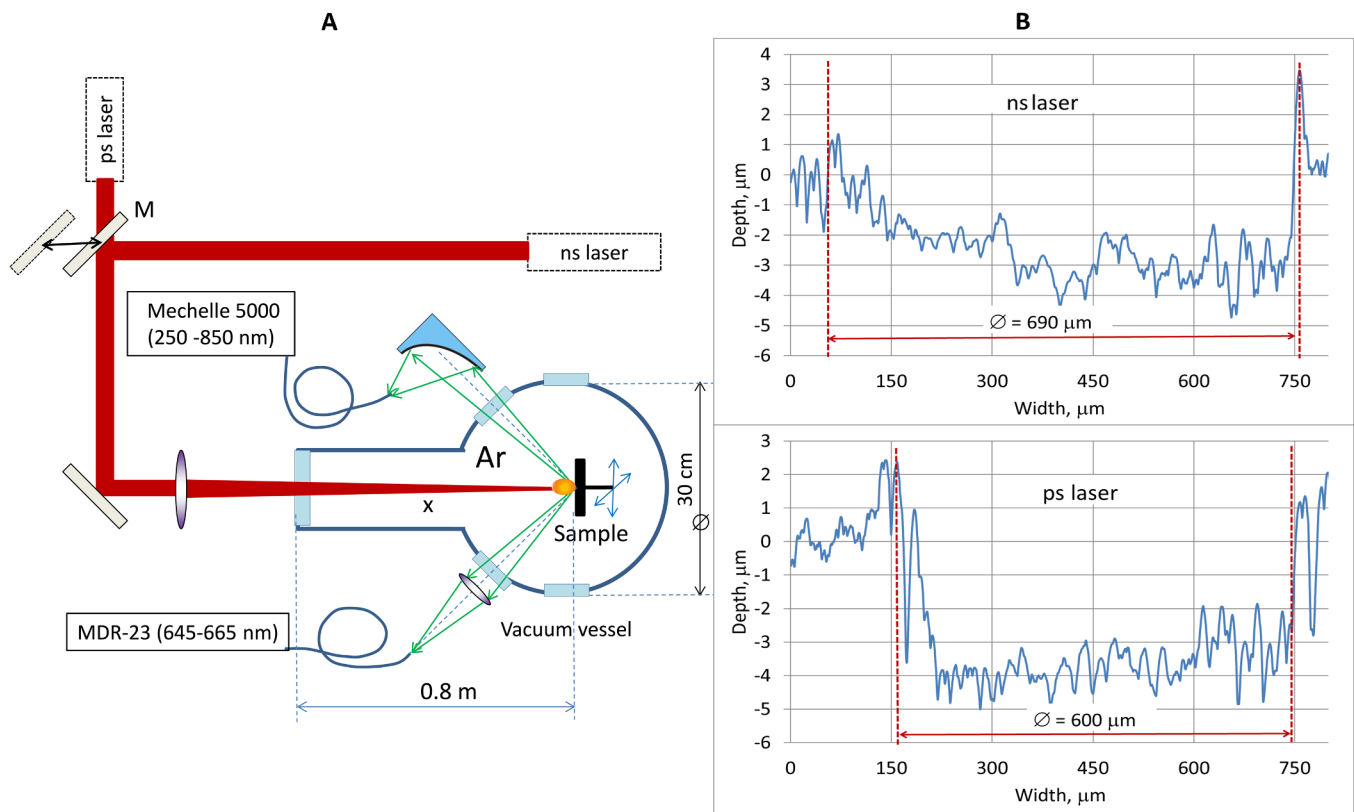


Fig. 1. A – sketch of the setup used in the experiments. B – profiles of craters formed by 30 laser pulses.

either “soft” or “hard” from the viewpoint of sputtering and ablation rate. Both types of coatings have been investigated in our previous studies [5] and it was found that only a small number of laser shots were needed to reach the substrate in case of “soft” W coatings with a thickness of a few micrometres. This complicates comparing the effect of laser pulse duration on the accuracy of D content determination and therefore we used here samples with a low ablation rate, prepared by Combined Magnetron Sputtering and Ion Implantation technique [6] which was successfully used to coat ITER-like walls [7]. Determination of elemental depth profiles by Gas Discharge Optical Spectrometry, GDOES, and Secondary Ion Mass Spectrometry, SIMS showed that the thickness of the coating was  $\approx 3 \mu\text{m}$  and contained  $\approx 10 \text{ at}\%$  of Al and  $\approx 5 \text{ at}\%$  of deuterium.

Experiments were carried out with the setup, Fig 1A, with more detailed description in [8]. The best S/N ratio was obtained by using argon at 300 Pa pressure as a background gas. Two Nd: YAG lasers with pulses of different durations (first from Ekspla with 0.15 ns pulses, and the second from Quantel with 8 ns pulses) lasing at 1064 nm, were used. The repetition rate of laser pulses was 1 Hz. The laser beam striking the target was changed by translating the mirror M as depicted in Fig. 1A. In both cases, the laser beam was focused onto the sample surface at  $90^\circ$  with the plano-convex lens of 1500 mm focal length.

A Mechelle 5000 (Andor) spectrometer was used for recording spectra in a broad range (250–850 nm) and MDR-23 for recording spectra in  $\approx 20 \text{ nm}$  range around the Balmer alpha lines of hydrogen isotopes. Both spectrometers recorded spectra at  $45^\circ$  with respect to the laser beam. The full width at half maximum, FWHM, of the instrumental function was determined with the help of a He:Ne laser. Spectrometers recorded time-gated spectra within a window of  $\Delta t = 2000 \text{ ns}$  using ICCD cameras.

To reach optimal conditions for reconstructing elemental depth profiles, the measurements were carried out at comparatively low values of laser pulse energies, 30–50 mJ and 10–20 mJ for ns and ps lasers, respectively. Spectra were recorded at different values of delay

time between the laser pulse and the beginning of data acquisition,  $t_d = 400\text{--}2000 \text{ ns}$ . At fixed values of  $t_d$  and laser energy, spectra belonging to thirty consequent laser shots were recorded from a number of different spots on the sample surface. The position of a new spot was set by shifting the sample holder. The distance between the spots was  $> 1.3 \text{ mm}$ . The depth profiles of craters were recorded by a 3D optical profiler New View 7100 (Zygo) and a Dektak 150 (Veeco Digital Instruments) contact profilometer, Fig. 1B. The structure of the crater bottom changed remarkably with the laser shot number and at a fixed shot number the roughness of the bottom of different craters was within  $0.5\text{--}1 \mu\text{m}$ . The diameter of craters produced by 30 laser shots was used for estimation of the average value of the laser fluence  $\Phi$  at the sample surface.

### 3. Results and analysis

Fig. 2 shows W depth profiles obtained by GDOES and LIBS. LIBS profile was found by using integral intensities of W lines at wavelengths of 653.24 and 653.81 nm. In case of LIBS profile, the main reason of a more gradual decay of the intensity is probably caused by the Gaussian distribution of the energy of laser beams as well as by the redeposition of the ablated material. The fitting of LIBS profile obtained by ps laser of  $\Phi = 5.5 \text{ Jcm}^{-2}$  fluence with the GDOES profile resulted in the value of coating ablation rate  $\approx 0.17 \mu\text{m}/\text{shot}$ . The ablation rate of the ns laser at  $\Phi = 10.6 \text{ Jcm}^{-2}$  was 1.7 times larger. Within the limits of the used laser energies, the ablation rate remained almost unchanged.

These values of ablation rates seem to contradict with the profile of 30-shot craters in Fig. 1B where the crater depths exceed only slightly the value of the coating thickness. This difference between depth profiles in Fig. 2 and crater profiles obtained by profilometer can be explained by a considerably lower ablation rate of the Mo substrate. Another factor reducing the Mo ablation rate is its higher value of the reflection coefficient at  $\lambda = 1064 \text{ nm}$  [9], which results in the absorbed energy being decreased.

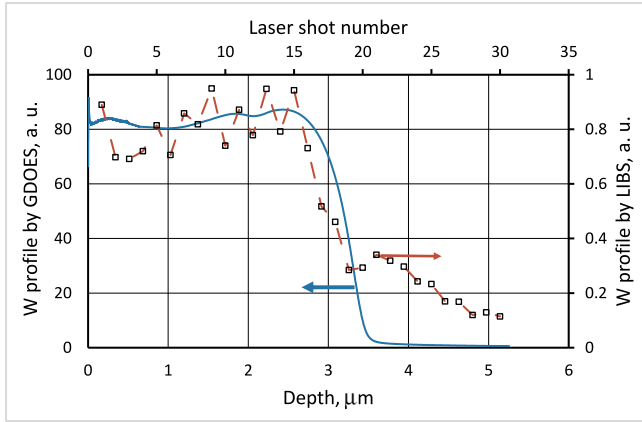


Fig. 2. Comparison of GDOES and LIBS profiles; ps laser,  $\Phi = 5.5 \text{ J cm}^{-2}$ . Ablation rate was obtained by fitting with GDOES profiles.

Fig. 3A presents an excerpt of the spectrum containing partly overlapping  $D_{\alpha}$  ( $\lambda = 656.09 \text{ nm}$ ) and  $H_{\alpha}$  ( $\lambda = 656.26 \text{ nm}$ ) lines. The main cycle of measurements was carried out at ns and ps laser energies where at a small number of laser shots,  $< 5$ ,  $H_{\alpha}$  peaks had comparable values. At  $t_d \geq 400 \text{ ns}$  and at smaller number of laser shots, the spectrum showed a two-humped structure, while for a larger number of shots,  $> 20$ , only the  $H_{\alpha}$  peak exceeded the noise level. As a common trend, the dip between  $D_{\alpha}$  and  $H_{\alpha}$  peaks was more pronounced at longer  $t_d$  values and at a fixed  $t_d$  the dip was more noticeable for ps laser.

At low background gas pressures, besides the instrumental broadening,  $\Gamma_I = 0.055 \text{ nm}$ , the FWHM of lines is also substantially influenced by Doppler and Stark effects. The line shapes corresponding to these mechanisms are given by Gaussian and Lorentzian profiles. Contours of these lines were fitted by pseudo Voigt functions using the least square method [10]. The Gaussian component of profiles was calculated from  $\Gamma_G = \sqrt{\Gamma_I^2 + \Gamma_D^2}$ . The FWHM of the Doppler broadening is  $\Gamma_D = 7.16 \times 10^{-7} \lambda_0 \sqrt{\frac{T}{M}}$  where  $M$  is mass in atomic mass units, temperature  $T$  in Kelvin results from Boltzmann plot, Fig. 5, and  $\lambda_0$  is the wavelength in nanometres. At  $t_d$  and  $\Phi$  values corresponding to those of Fig. 5,  $\Gamma_D$  values of ns laser for  $D_{\alpha}$  ja  $H_{\alpha}$  lines were 0.056 and 0.079 nm, respectively. The FWHM of the Lorentzian component,  $\Gamma_L$ , was used as a fitting parameter. Its initial value was found by fitting Voigt contours with spectra showing only the  $H_{\alpha}$  line, Fig. 3A. Delay times  $t_d \geq 800 \text{ ns}$  resulted in reasonable separation of  $D_{\alpha}$  and  $H_{\alpha}$  peaks by curve-fitting and  $\Gamma_L = 0.07\text{--}0.08 \text{ nm}$  was obtained for both lasers. The S/N ratio of  $D_{\alpha}$  and  $H_{\alpha}$  peaks was reasonably high even at higher delay times when MDR spectrometer was used. The fitting was used to

calculate the intensities of  $D_{\alpha}$  and  $H_{\alpha}$  lines as well as the background level BG. The main factor influencing the accuracy of  $D_{\alpha}$  determination was the overlapping by the more intensive  $H_{\alpha}$  line. For spectrum presented in Fig. 2B the relative standard errors, RSE, of fits for  $D_{\alpha}$  and  $H_{\alpha}$  lines were  $\approx 6\%$  and  $\approx 1.5\%$ , respectively. Under the same general conditions, RSE of the fit for ns laser spectrum was larger by a factor of two when compared with the ps laser spectra.

The S/N ratio for tungsten lines recorded by the Mechelle 5000 spectrometer was too low at  $t_d > 800 \text{ ns}$  and further data processing was carried out for results obtained at  $t_d = 800 \text{ ns}$ . In spite of a good fitting of single-shot  $D_{\alpha}/H_{\alpha}$  spectra by Voigt functions, shot-to-shot intensities of spectral lines fluctuated remarkably. The main reason of fluctuations was probably the roughness of the crater structure, Fig. 1B, which changed randomly from shot to shot thus influencing the amount of ablated matter and intensity of spectral lines. Averaging spectra over a number of spots [11] diminished the extent of fluctuations.

Fig. 4 demonstrates a satisfactory coincidence of  $D_{\alpha}$  and W profiles and the matching of these profiles with the Mo profile.

The use of Lorentzian FWHM of  $\alpha$ -lines of hydrogen isotopes and a set of W lines allowed to evaluate the electron density  $n_e$  and the electron temperature  $T_e$  of the plasma plume formed during the first 5–10 laser shots.

Assuming local thermal equilibrium, LTE, the electron temperature  $T_e$  could be found from the slope of the linear dependence (Boltzmann plot)  $\ln [I/A_{ki}g_k] = f(E_k)$  [12]. Here  $I$  is the intensity of a spectral line,  $A_{ki}$  is the radiative transition probability of the corresponding transition,  $g_k$  and  $E_k$  are statistical weight and energy of the upper state, respectively. The validity of the LTE was estimated on the basis of Mc Whirter criterion. In the worst case, the estimated electron density exceeded the criterion 1.8 times.

W lines were selected according to considerations described in [13], excluding lines with higher values of self-absorption. In the wavelength range 330–520 nm, 19 lines from spectra obtained by ps laser and 16 lines from those of ns laser were chosen and characterized by integral intensities. The deviation of points from the straight line is comparatively small according to Fig. 5 and the analysis showed that in the case of ps laser the effect of self-absorption is slightly smaller. Slopes of trendlines in Fig. 5A gave  $T_e = 0.85 \text{ eV}$  (9800 K) for the ns laser and  $T_e = 0.75 \text{ eV}$  (8700 K) for the ps laser. Because of the lower intensity of W lines in the ps laser spectra, the intercept of the corresponding Boltzmann plot has  $\approx 1.4$  times smaller value than that of the ns laser. When the coating was removed due to ablation, Mo lines were used for  $T_e$  estimation. The list of the selected 13 Mo lines did not contain intensive lines with transition to the ground state. The difference between temperatures found from measurements with ns and ps lasers was within the uncertainty of measurements and the average temperature

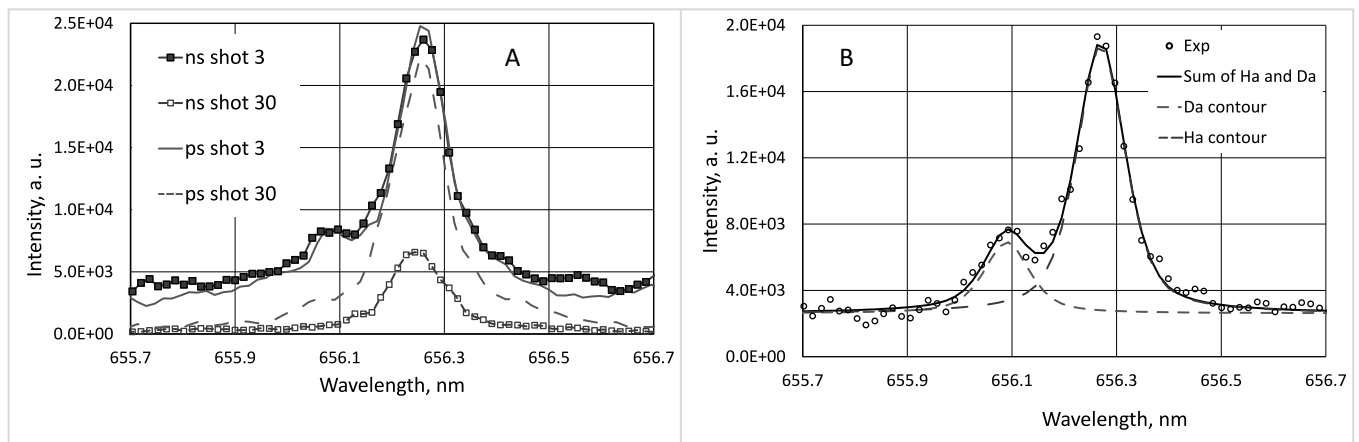


Fig. 3. A – Spectra of hydrogen isotopes; ns laser  $\Phi = 10.6 \text{ J cm}^{-2}$ , ps laser  $\Phi = 5.5 \text{ J cm}^{-2}$ ;  $t_d = 800 \text{ ns}$ ; B – fitting by Voigt profiles; ps laser  $\Phi = 5.5 \text{ J cm}^{-2}$ ;  $t_d = 1600 \text{ ns}$ . Presented spectra belong to single spots.

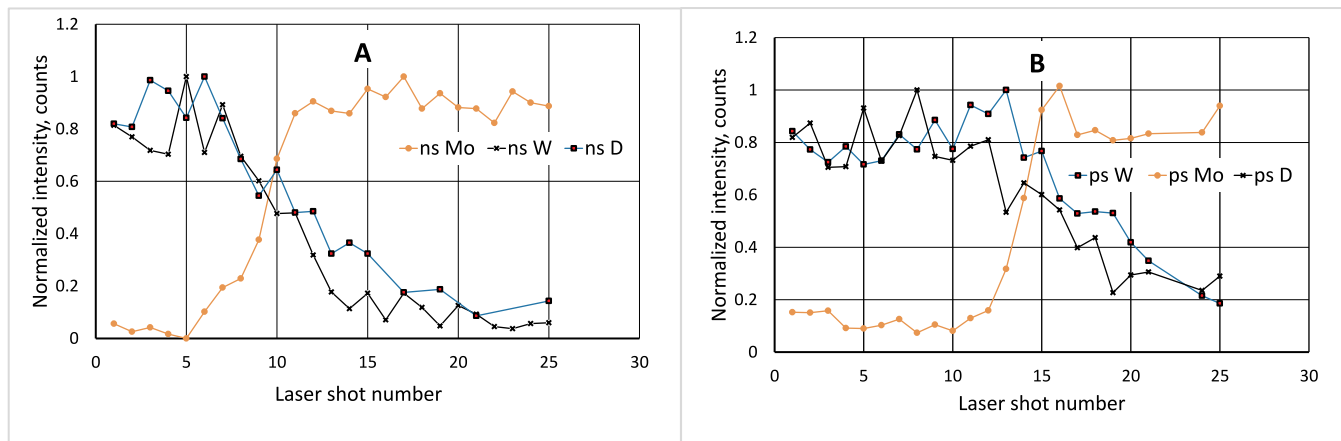


Fig. 4. LIBS profiles of  $D_{\alpha}$ , W and Mo;  $t_d = 800 \text{ ns}$ . A – ns laser,  $\Phi = 10.6 \text{ J cm}^{-2}$ . B – ps laser;  $\Phi = 5.5 \text{ J cm}^{-2}$ . Profiles result the averaging over 3 spots.

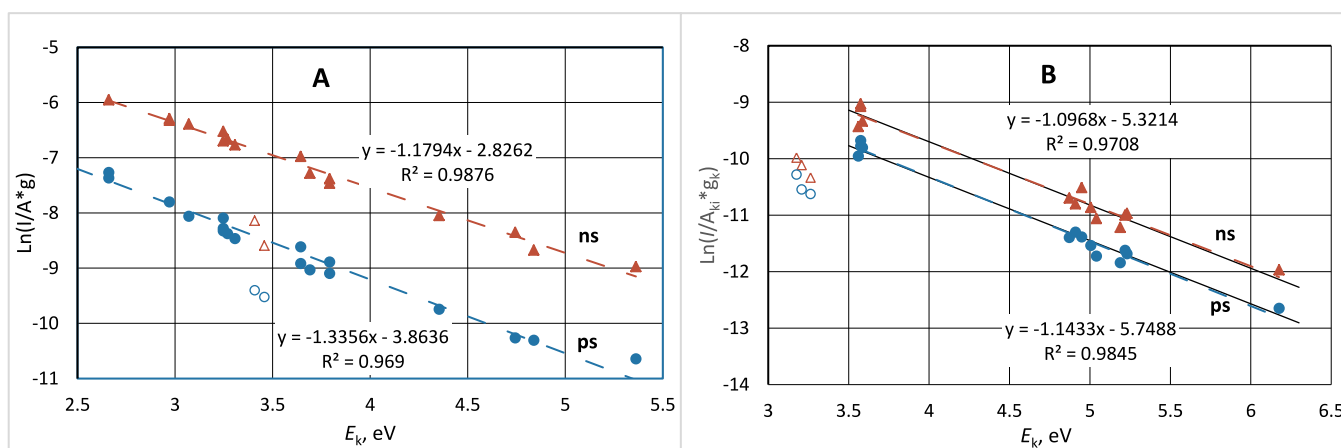


Fig. 5. Boltzmann plots;  $t_d = 800 \text{ ns}$ ; ps laser  $\Phi = 5.5 \text{ J cm}^{-2}$ ; ns laser  $\Phi = 10.6 \text{ J cm}^{-2}$ . A - shot 2; intensities of W lines with corresponding trendlines; open symbols belong to lines with a strong self-absorption, 400.9 and 407.4 nm. B - shot 20; intensities of Mo lines; dashed lines are trendlines; solid lines correspond to the temperature 0.89 eV; open symbols belong to lines with a strong self-absorption, 379.8, 386.4 and 390.3 nm.

was 0.89 eV (10,360 K), Fig. 5B.

The value for electron density,  $n_e \approx 2 \times 10^{15} \text{ cm}^{-3}$  was obtained from the Lorentzian FWHM of  $H_{\alpha}$  line with the help of the relationship  $\Gamma_L = 4.63 \times 10^{-12} n_e^{2/3}$  presented in [14].

It is interesting to compare our findings with other similar studies. In [15] an overview of experimental studies of ablation with lasers of different pulse durations as well as the results of a detailed modelling are presented. Similarly to our results, both experiments and modelling show that at longer delay times,  $t_d > 100 \text{ ns}$ , the plasma characteristics depend on the total energy deposited and not on the pulse duration. Reference [16] showed that at a fixed laser wavelength and energy the ablation efficiency,  $\text{cm}^3 \text{ J}^{-1}$ , of a ns laser is by a factor 5 larger than that of a ps laser. Smaller amount of evaporated material could be a reason why in our ps laser measurements the self-absorption effects are less pronounced.

#### 4. Conclusions

LIBS spectra produced by lasers of 0.15 and 8 ns pulse durations were recorded. Experiments with ITER-relevant samples were carried out at low values of laser fluence  $\Phi$  which allowed a reliable design of depth profiles of deuterium and tungsten. The main factor limiting the accuracy of curve-fitting of deuterium line was the high-intensity hydrogen signal.

Comparison with ns laser permits to carry out the following advantages of ps laser

- Almost the same intensity of  $\alpha$ -lines of hydrogen isotopes was achieved at two times lower values of laser fluence, while the intensity of W lines was much lower
- RSE of the curve-fitting of  $D_{\alpha}$  profile was two times lower
- Intensities of W lines were less influenced by self-absorption which important from the viewpoint of application of CF LIBS

The drawback of the used values of fluence was a comparatively low value of the S/N ratio and thus the observed features of ps laser are just trends. Testing of thicker ITER-relevant coatings together with higher values of fluence gives a possibility to carry out the specificity of ps laser more definitely. Furthermore, using higher values of fluence decrease the shot noise governing the S/N ratio at longer delay times which is used in LIBS measurements at near-atmospheric pressures of the background gas. In these conditions however the strong hydrogen signal could shadow the reliable determination of deuterium.

#### Acknowledgements

This work has been carried out within the framework of the EUROfusion Consortium and has received funding from the European Union's Horizon 2020 research and innovation programme under grant agreement number 633053. The views and opinions expressed herein do not necessarily reflect those of the European Commission. Work performed under EUROfusion WP PFC.

## References

- [1] A. Ciucci, M. Corsi, V. Palleschi, S. Rastelli, A. Salvetti E. Tognoni, New procedure for quantitative elemental analysis by laser-induced plasma spectroscopy, *Appl. Spectrosc.* 53 (1999) 960–964.
- [2] S. Almaviva, L. Caneve, F. Colao, G. Maddaluno, N. Krawczyk, A. Czarnecka, P. Gasiot, M. Kubkowska, M. Lepek, Measurements of deuterium retention and surface elemental composition with double pulse laser induced breakdown spectroscopy, *Phys. Scr.* T167 (2016) 014043.
- [3] P. Stavropoulos, C. Palagas, G.N. Angelopoulos, D.N. Papamantellos, S. Couris, Calibration measurements in laser-induced breakdown spectroscopy using nanosecond and picosecond lasers, *Spectrochim. Acta B* 59 (2004) 1885–1892.
- [4] V. Morel, B. Pérès, A. Bultel, A. Hideur, C. Grisolia, Picosecond LIBS diagnostics for Tokamak in situ plasma facing materials chemical analysis, *Phys. Scr.* T167 (2016) 014016.
- [5] M. Laan, A. Hakola, P. Paris, K. Piip, M. Aints, I. Jögi, J. Kozlova, H. Mändar, C. Lungu, C. Porosnicu, E. Grigore, C. Ruset, J. Kolehmainen, S. Tervakangas, Dependence of LIBS spectra on the surface composition and morphology of W/Al coatings, *Fusion Eng. Des.* 121 (2017) 296–300.
- [6] C. Ruset, E. Grigore, H. Maier, R. Neu, X. Li, H. Dong, R. Mitteau, X. Courtois, JET EFDA contributors, tungsten coatings deposited on CFC tiles by the combined magnetron sputtering and ion implantation technique, *Phys. Scripta* T128 (2007) 171–174.
- [7] C. Ruset, E. Grigore, H. Maier, R. Neu, H. Greuner, M. Mayer, G. Matthews, Development of W coatings for fusion applications, *Fusion Eng. Des.* 86 (2011) 1677–1680.
- [8] P. Paris, J. Butikova, M. Laan, M. Aints, A. Hakola, K. Piip, I. Tufail, P. Veis, Detection of deuterium retention by LIBS at different background pressures, *Phys. Scr.* T170 (2017) 014003.
- [9] M. Joanny, J.M. Travère, S. Salasca, L. Marot, E. Meyer, C. Thellier, C. Cammarata, G. Gallay, J.J. Fermé, Achievements on engineering and manufacturing of ITER first-mirror mock-ups, *IEEE Trans. Plasma Sci.* 40 (2012) 692–696.
- [10] T. Ida, M. Ando, H. Toraya, Extended pseudo-Voigt function for approximating the Voigt profile, *J. Appl. Cryst.* 33 (2000) 1311–1316.
- [11] P. Paris, M. Aints, A. Hakola, M. Kiisk, J. Kolehmainen, M. Laan, J. Likonen, C. Ruset, K. Sugiyama, S. Tervakangas, Determination of elemental depth profiles by multi-spot averaging technique of LIBS spectra, *Fusion Eng. Des.* 86 (2011) 1125–1128.
- [12] D.W. Hahn, N. Omenetto, Laser-induced breakdown spectroscopy (LIBS), part II: review of instrumental and methodological approaches to material analysis and applications to different fields, *Appl. Spectrosc.* 66 (2012) 347–419.
- [13] A. Lissovski, K. Piip, L. Hämarik, M. Aints, M. Laan, P. Paris, A. Hakola, J. Karhunen, LIBS for tungsten diagnostics in vacuum: selection of analytes, *J. Nuclear Mater.* 463 (2015) 923–926.
- [14] R. Fantoni, S. Almaviva, L. Caneve, F. Colao, A.M. Popov, G. Maddaluno, Development of calibration-free laser-Induced-Breakdown Spectroscopy based techniques for deposited layers diagnostics on ITER-like tiles, *Spectrochim. Acta B* 87 (2013) 153–160.
- [15] A. Bogaerts, Z. Chen, Effect of laser parameters on laser ablation and laser-induced plasma formation: a numerical modeling investigation, *Spectrochim. Acta B* 60 (2005) 1280–1307.
- [16] A. Semerok, C. Chaleard, V. Detalle, J.-L. Lacour, P. Mauchien, P. Meynadier, C. Nouvellon, B. Salle, P. Palianov, M. Perdrix, G. Petite, Experimental investigations of laser ablation efficiency of pure metals with femto, pico and nanosecond pulses, *Appl. Surf. Sci.* 138–139 (1999) 311–314.

Institute of Solid State Physics, University of Latvia as the Center of Excellence has received funding from the European Union’s Horizon 2020 Framework Programme H2020-WIDESPREAD-01-2016-2017-TeamingPhase2 under grant agreement No. 739508, project CAMART<sup>2</sup>